Heterogeneous and Complex Rearrangements of Chromosome Arm 6q in Chondromyxoid Fibroma Delineation of Breakpoints and Analysis of Candidate Target Genes

Romeo, S.; Duim, R.A.J.; Bridge, J.A.; Mertens, F.; Jong, D. de; Cin, P. dal; ... ; Hogendoorn, P.C.W.

The American Journal of Pathology, Vol. 177, No. 3, September 2010

DOI: 10.2353/ajpath.2010.091277

Molecular Pathogenesis of Genetic and Inherited Diseases

Heterogeneous and Complex Rearrangements of Chromosome Arm 6q in Chondromyxoid Fibroma

Delineation of Breakpoints and Analysis of Candidate Target Genes

Salvatore Romeo,* Ronald A.J. Duim,* Julia A. Bridge,† Fredrik Mertens,‡ Danielle de Jong,§ Paola Dal Cin,¶ Pauline M. Wijers-Koster,* Maria Debiec-Rychter,‖ Raf Sciot,** Andrew E. Rosenberg,†† Karoly Szuhai,§ and Pancras C.W. Hogendoorn*

From the Departments of Pathology, and Molecular Cell Biology,§ Leiden University Medical Center, Leiden, The Netherlands; the Departments of Pathology/Microbiology, Pediatrics, and Orthopaedic Surgery,† University of Nebraska Medical Center, Omaha, Nebraska; the Department of Clinical Genetics,‡ Lund University Hospital, Lund, Sweden; the Department of Pathology,¶ Brigham and Women's Hospital, Boston, Massachusetts; the Department of Human Genetics‖ and Pathology,** Catholic University of Leuven, Leuven, Belgium; and the Department of Pathology,†† Massachusetts General Hospital, Boston, Massachusetts*

Chondromyxoid fibroma (CMF) is an uncommon benign cartilaginous tumor of bone usually occurring during the second decade of life. CMF is associated with recurrent rearrangements of chromosome bands 6p23–25, 6q12–15, and 6q23–27. To delineate further the role and frequency of the involvement of three candidate regions (6q13, 6q23.3 and 6q24) in the pathogenesis of CMF, we studied a group of 43 cases using a molecular cytogenetic approach. Fluorescence *in situ* hybridization with probe sets bracketing the putative breakpoint regions was performed in 30 cases. The expression level of nearby candidate genes was studied by immunohistochemistry and quantitative RT-PCR in 24 and 23 cases, respectively. Whole-genome copy number screening was performed by array comparative genomic hybridization in 16 cases. Balanced and unbalanced rearrangements of 6q13 and 6q23.3 occurred in six and five cases, respectively, and a hemizygous deletion in 6q24 was found in five cases. Two known tumor suppressor genes map to the latter region: *PLAGL1* and *UTRN*. However, neither of these two genes nor *BCLAF1* and *COL12A1*, respectively located in 6q23.3 and 6q13, showed altered expression. Therefore, although rearrangements of chromosomal regions 6q13, 6q23.3, and 6q24 are common in CMF, the complexity of the changes precludes the use of a single fluorescence *in situ* hybridization probe set as an adjunct diagnostic tool. These data indicate that the genetic alterations in CMF are heterogeneous and are likely a result of a cryptic rearrangement beyond the resolution level of combined binary ratio fluorescence *in situ* hybridization or a point mutation. ***(Am J Pathol 2010, 177:1365–1376; DOI: 10.2353/ajpath.2010.091277)***

Chondromyxoid fibroma (CMF) is an uncommon, benign, morphologically unique cartilaginous tumor of bone. Histologically, it is composed of spindle and stellate cells embedded in a myxo-chondroid matrix.[1,2] The pathological features of CMF have been shown to resemble the morphological changes displayed during *in vitro* chondrogenesis and are well recognized to cause diagnostic challenges with chondrosarcoma.[3,4] The immunohistochemical assessment of CDKN2A (p16/INK4A), CCND1, and ALCAM, which evaluates cell-cycle regulation and

Supported by EuroBoNeT, a European Community granted network of excellence for studying the pathology and genetics of bone tumors (grant LSHC-CT-2006-018814). S.R., R.A.J.D., F.M., D.J., P.M.W.K., M.D.R., R.S., K.S., and P.C.W.H. are partners within EuroBoNeT.

Accepted for publication May 27, 2010.

This work was presented at the 99th Annual Meeting of the United States and Canadian Academy of Pathology, March 20–26, 2010, Washington, DC.

Current address of S.R.: Pathology, Treviso Regional Hospital, Treviso, Italy.

Address reprint requests to Pancras C.W. Hogendoorn, M.D., Ph.D., Department of Pathology, Leiden University Medical Center, P.O. Box 2300, RC Leiden, The Netherlands. E-mail: P.C.W.Hogendoorn@lumc.nl.

cell-cell adhesions mechanisms active in these tumors, might be a promising tool for such a task.[5]

The genetic mechanism underlying the pathogenesis of CMF remains poorly understood, although recurrent cytogenetic findings have implicated gene(s) on chromosome 6. To date, 22 cases of CMF with aberrant karyotypes have been reported in literature, and the abnormalities have included both balanced and unbalanced rearrangements (Mitelman Database of Chromosome Aberrations in Cancer, *http://cgap.nci.nih.gov/Chromosomes/* 2009, last accessed on December 23, 2009).[6–9] In 18 of these cases, several bands on chromosome 6, notably 6p25, 6q13, 6q15, 6q23, and 6q25, have been involved.[6–8] An apparently identical inv(6)(p25q13) has been described as the sole abnormality in two cases.[10,11] The majority of changes have been complex rearrangements and delineation of the breakpoints has been performed mainly at the resolution level of conventional cytogenetics, with spectral karyotyping used in a few cases, and fluorescence *in situ* hybridization (FISH) mapping used in one case (Mitelman Database of Chromosome Aberrations in Cancer, *http://cgap.nci.nih.gov/Chromosomes/* 2009)[6–8,12] In the present study, we analyzed the genetic changes involving chromosome 6 in a group of CMFs to characterize the breakpoints and search for possible candidate target genes and the roles they may play in the pathogenesis of this tumor.

Materials and Methods

Patients

Forty-three cases with the histological features of CMF were collected. Clinical data and tests performed are shown in Table 1. All samples were handled in a coded fashion, and all procedures were performed according to the ethical guidelines in Code for Proper Secondary Use of Human Tissue in the Netherlands (Dutch Federation of Medical Scientific Societies).

Cytogenetic Methods

Cells from 22 tumor samples were available for culture and chromosome banding analysis. Cell culture, harvest conditions, and karyotyping were performed according to standard protocols.[13]

Combined Binary Ratio Fluorescence in Situ *Hybridization (COBRA-FISH)*

Multicolor COBRA-FISH was performed on metaphase spreads from five cases (CMF22, CMF28, CMF29,CMF31 and CMF43), using methods previously described.[14] Hybridizations with individual BAC probes and whole chromosome painting (wcp) labeled with single fluorochromes were used to confirm the detected rearrangements. Chromosomal breakpoints were assigned by using inverted 4′,6-diamidino-2-phenylindole (DAPI; Downers Grove, IL) counterstained images together with the information derived from the short and long arm–specific hybridizations. Karyotypes were described according to ISCN 2009.

Array Comparative genomic Hybridization (CGH)

DNA was isolated from 15 snap-frozen tissue samples containing >70% tumor cells as estimated by hematoxylin and eosin staining, and from primary cultured cells from CMF31. A Wizard genomic DNA purification kit (Promega, Madison, WI) was used according to the manufacturer's instructions. The test and gender matched reference samples were labeled using BioPrime total labeling kit (Invitrogen, Breda, The Netherlands) incorporating indocarbocyanine-deoxycytidine triphosphates (Cy3-dCTP; GE Health Care Europe GmbH, Diegem, Belgium) and indodicarbocyanine (Cy5-dCTP (GE Health Care), respectively. The reference material used was commercially available DNA samples (Promega). Labeled samples were pooled and hybridized on an in-house printed array chip with 1 Mbp resolution, containing large genomic insert clones (BAC, PAC, cosmid, and fosmid) provided by the group of Dr. Nigel Carter, Welcome Trust Sanger Institute (Cambridge, UK). Information regarding the full set is available at the database of the Wellcome Trust Sanger Institute: Ensembl (*http://www.ensembl.org/* last accessed on December 23. 2009). Array printing, hybridization, image acquisition procedures, data extraction, and normalizations were performed as previously described.[15,16] Further analysis and averaging of the triplicate spotted clones was performed with CGH Analyzer MeV (University of Pennsylvania, Abramson Cancer Research Institute).[17]

FISH Mapping

Large genomic insert clones (BACs, PACs) (Wellcome Trust Sanger Institute, Cambridge, UK) and fosmid clones (University of Santa Cruz California, CA) flanking the 6q23 and 17p13 breakpoint regions in CMF22 were labeled with fluorescein isothiocyanate or Cy3 dUTP using a BioPrime random prime labeling kit (Invitrogen) according to the manufacturer's instructions, with slight modifications.[16] Hybridization was performed on metaphase slides as previously described.[16]

Interphase and Metaphase FISH for 6q13, 6q23.3, 6q24, and 17p13.3

For the investigation of the three involved regions on chromosome 6 several FISH probe sets were used (Table 2). Three candidate breakpoint regions in chromosome bands 6q13, 6q23.3, and 6q24 were evaluated by FISH in 30 cases. For 6q13, probe sets previously reported were used,[8] and for 6q23.3 two probe sets flanking the breakpoint occurring in CMF22 were used (Table 2). For the 6q24 region, which was found to be commonly deleted in our array CGH experiments, two probes flanking

Table 1. Clinical Data and Analyses Performed on a Series of 43 CMF

Name	L number	Age	Sex	Location	Array CGH	qRT-PCR	IHC	Karyotyping	6q13, 6q23.3, 6q24 FISH
CMF1*		20	M	Femur			+		
CMF2*	1363	14	M	Phalanx	+	+	+		I
CMF3*	1105	15	M	Metatarsus	+	+	+		I
CMF4*		49	M	Tibia			+		
CMF5*	148	16	M	Metatarsus		+	+		
CMF6*		34	F	Ulna			+		
CMF7*		8	M	Tibia			+		
CMF8*		7	M	Femur			+		
CMF9*	1362	60	F	Os ilium	+	+	+		I
CMF10*		35	F	Tibia			+		
CMF11*	938	10	F	Metatarsus	+	+	+		I
CMF12*		15	M	Tibia			+		
CMF13*	359	63	M	Tibia	+	+	+		I
CMF14*		9	F	Tibia			+		
CMF15*		27	M	Metatarsus			+		
CMF16*		29	F	Os ilium			+		
CMF17*		23	M	Femur			+		
CMF18*		41	F	Rib			+		
CMF19*	1365	39	M	Sternum	+	+	+		I
CMF20*	1252	12	F	Femur	+	+	+		I
CMF21	1787	14	M	Tibia	+	+	+	+	I
CMF22	1788	20	F	Os ilium	+	+	+	+	M
CMF23	1789	50	F	Os ilium	+	+	+		I
CMF24	1790	19	M	Femur	+	+	+		I
CMF25	1913	15	F	Tibia	+	+		+	I
CMF26	1951	12	M	Tibia	+	+		+	I
CMF27	2001	57	M	Os ischium	+	+		+	I
CMF28	2367	13	M	Tibia	+	+		+	I and M
CMF29	2499	53	M	Femur				+	M
CMF30	2514	12	M	Tibia				+	I
CMF31	2515	4	M	Tibia	+			+	M
CMF32† (case 1)	2634	29	M	Tibia		+		+	I
CMF33† (case 3a)	2631	61	F	Os ilium		+		+	I
CMF34† (case 4)		10	M	Humerus				+	I
CMF35† (case 5)	2632	21	F	Os ilium		+		+	I
CMF36† (case 6)	2630	12	M	Tibia		+		+	I
CMF37† (case 7)	2633	23	M	Os ilium		+		+	I
CMF38† (case 8b)	2628	55	F	Tibia		+		+	I
CMF39† (case 9)		37	F	Femur				+	
CMF40† (case 10)		13	M	Os ilium				+	
CMF41† (case11)		44	F	Ulna				+	
CMF42† (case12)	2629	55	M	Tibia		+		+	I
CMF43		46	M	Os ilium				+	M

*Cases previously reported (5).
†Cases previously reported[9] between brackets; the case number as reported before.[9]
M, male; F, female; IHC, immunohistochemistry; I, interphase; M, metaphase; NA, not available.

UTRN were used (Table 2); this tumor suppressor gene is known to be deleted in several types of neoplasms.[18] FISH was performed on interphase nuclei in 26 cases, on metaphase spreads in five (CMF22, CMF28, CMF29, CMF31 and CMF43), and on both interphase nuclei and metaphase spreads in one tumor (CMF29), giving consistent results. Probe labeling and hybridization were done as previously described.[16] For the evaluation of 6q13 rearrangements two sets of probes flanking the region were used: RP11-536O4, RP11-560O20, and RP1-238D15 (red signal, proximal region) and RP11-209D8 and RP1-234P15 (green signal, distal region) (Table 2). For the evaluation of 6q23.3 rearrangements two probes sets were used: 1. RP11-422G24 (red signal, proximal to the region) and RP13-143G15 (green signal, distal region), this set was used for metaphase experiments, and 2. WI2-642E16 (G248P8982C8) (red signal, proximal region) and WI2-2673O18 (G248P8342H9) (green signal, distal region), this set was used for interphase experiments (Table 2). Cases harboring 6q23.3 translocation were further investigated for rearrangements in 17p13.3 with an additional FISH experiment using a co-localization probe set for the 17p region containing the *GARNL4* gene and the 6q23.3 probe (Table 2). For the evaluation of 6q24 rearrangements two probes flanking the region were used: RP11-352E13 (red signal, distal region) and RP11-737K07 (green signal, proximal region) (Table 2); in addition, a third probe for the centromere of chromosome 6 (α satellite DNA CEP6) was applied (blue signal).

Slides were evaluated with a Leica RD1000 epifluorescence microscope. For interphase FISH, 200 nuclei per case were scored. The cut-off point was set at 5% based on scores obtained on normal tissue slides.

Table 2. Overview of the Probes Used for Interphase and Metaphase FISH

Clone name	Chromosome	Band	Start	End	Gene of interest	Label
RP11-536O4*	6	q13	75,650,864	75,770,821	*COL12A1*	Red
RP11-560O20*	6	q13	75,449,686	75,650,863	*COL12A1*	Red
RP1-238D15*	6	q13	75,770,822	75,881,113	*COL12A1*	Red
RP11-209D8*	6	q13	75,832,221	75,998,902	*COL12A1*	Green
RP1-234P15*	6	q13	75,891,220	76,016,760	*COL12A1*	Green
RP11-422G24*	6	q23.3	136,621,876	136,828,683	*BCLAF1*	Red
WI2-2673O18 (G248P8342H9)†	6	q23.3	136,661,677	136,706,538	*BCLAF1*	Red
WI2-642E16 (G248P8982C8)†	6	q23.3	136,603,323	136,648,311	*BCLAF1*	Green
RP13-143G15*	6	q23.3	136,288,787	136,422,604	*BCLAF1*	Green
RP11-352E13*	6	q24	145,129,550	145,330,848	*UTRN*	Red
RP11-737K07*	6	q24	144,334,917	144,527,085	*UTRN*	Green
RP11-74E22*	17	p13.3	2,545,429	2,705,380	*GARNL4*	Red
RP11-229E07*	17	p13.3	2,820,297	2,820,297	*GARNL4*	Green

*According to release 55 at *http://www.ensembl.org*.
†According to hg18 at *http://genome.ucsc.edu*.

Long-Range PCR

FISH mapping in CMF22 predicted the location of the translocation breakpoints in 6q23.3 and 17p13.3 to two 30- to 40-kbp regions. Forward and reverse primers were designed for every 5 kbp within these two chromosomal regions. Several primer pair combinations were tested to detect translocation for both derivative chromosome regions using long-range PCR approach (Table 3). Primers were paired to give a product only when the translocated regions were juxtaposed. Primer combinations resulting in amplicons of 10 kbp and 5 kbp from 6q23.3 and 17p13.3 were used as positive controls to check the efficiency of the reaction. PCR reactions were performed in a GeneAmp PCR system 9700 (Applied Biosystems, Foster City, CA) on 50 ng of DNA (extracted from CMF22) in a 25-μl reaction containing 10 pmol of each primer, 5 μl of Phusion GC buffer (Finnzyme, Keilaranta, Finland), and 0.5 unit of Phusion DNA polymerase (Finnzyme). Two types of negative controls were used: either no template control or DNA isolated from human placenta not harboring the t(6;17)(q23;p13). PCR products were analyzed on a 1% agarose gel.

Cloning, Sequencing, and Confirmatory Genomic PCR

Products from long-range PCR were cloned in pGEM-T Easy vector systems (Promega) according to the manufacturer's instructions. Plasmid DNA from bacteria was isolated with QIAprep Spin Miniprep kit (Qiagen, Venlo, The Netherlands) according to the manufacturer's in-

Table 3. Sequences of the Primers Used

Primers for long-range PCR			
Chromosome	strand	Start–end	Sequence
6	+	136,645,303–136,645,324	5′-CAAAGCTTCGGACCACATCATT-3′
17	+	2,660,001–2,660,022	5′-GGAGTTGGGGATGTGAGTGTCA-3′
Primers for genomic PCR			
Chromosome	strand	Start–end	Sequence
6	+	136,646,695–136,646,716	5′-AAGCCAAGCAAGATTGGGTACA-3′
17	+	2,666,846–2,666,866	5′-ATTCCCTCATCTCCACAGCAC-3′
Primers for RT-PCR			
Gene	Accession number	Forward primer	Reverse primer
GARNL4	NM_015085	5′-GGATGGATCGACAAGACCAT-3′	5-TCTCAAAGAACTCCGACGACT-3′
BCLAF1	NM_014739	5′-CGCGTCGAAGGTAGCTCTAT-3′	5′-TTGGAGCGACCCATTTCTTTT-3′
Primers for Q PCR			
Gene	Accession number	Forward primer	Reverse primer
GARNL4	NM_015085	5′-TACACAACATTCCGGGACAG-3′,	5′-AGGCTATCATGTCTGGGACAA-3′
BCLAF1	NM_014739	5′-ACGAGCGGTTCACTTCGTATAT-3′	5′-TGCTAAACGGGTATGCTTCC-3′
UTRN	NM_007124.2	5′-GGAGCAGGATGATATTTCTGATG-3′	5′-CTTCGTCTGACAGAGTTCCTTGT-3′
PLAGL1	NM_001080952	5′-AGCCGTTGCTCACAGCTCAG-3′	5′-AGCAGCCACATTAGACGTGA-3′
*GPR108**	XM_290854	5′-AGATGCCCCTTTTCAAGCTCTAC-3′	5′-GCCATGAGCCAGTGGATCTTG-3′
*HNRPH1**	NM_005520	5′-GATGTAGCAAGGAAGAAATTGTTCAG-3′	5′-CACCGGCAATGTTATCCCAT-3′
*CAPNS1**	NM_001749	5′-ATGGTTTTGGCATTGACACATG-3′	5′-GCTTGCCTGTGGTGTCGC-3′

Start–end base pair position according to hg18 at *http://genome.ucsc.edu*.
*Genes used for normalization.

structions. Sequencing was performed using primers from the long-range PCR reactions and the ABI Prism BigDye terminator cycle sequencing ready reaction kit according to the manufacturer's recommendations (Perkin-Elmer Applied Biosystems). Both strands were sequenced. Samples were run on an ABI 377 semiautomated sequencer (Perkin-Elmer).

New primers were designed to amplify the rearranged DNA within a smaller fragment (~500 bp). PCR reactions were conducted using the GeneAmp PCR system 9700 (Applied Biosystems, Foster City, CA) on 20 ng of DNA in a 25-μl reaction containing 10 pmol of each primer, 3 μmol/L $MgCl_2$, 1X PCR buffer II, and 0.5 unit of AmpliTaq (Roche, Basel, Switzerland). Positive control reactions were similarly set as for long-range PCR: primers combinations resulting in amplicons of 500 bp from 6q23.3 and 17p13.3 were used as positive controls. Two types of negative controls were used: either no template control or DNA isolated from human placenta not harboring the t(6;17)(q23;p13). PCR products were analyzed on a 1.5% agarose gel.

Search for Fusion mRNA by RT-PCR and 5′ RACE PCR

Based on the long-range PCR and sequencing results, primers were designed to detect possible RNA fusion products resulting from the balanced translocation in CMF22. In addition, different primer combinations were designed to amplify transcribed products from wild-type alleles. Total RNA was extracted from snap-frozen tissue of CMF22 and cDNA for RT-PCR synthesized as previously described.[5] RT-PCR reactions were performed using the GeneAmp PCR system 9700 (Applied Biosystems) on 0.4 μl of cDNA in a 25-μl reaction containing 10 pmol of each primer, 3 μmol/L $MgCl_2$, 1X PCR buffer II, and 0.5 unit of AmpliTaq (Roche). For RACE PCR, cDNA synthesis and amplification were performed with the SMART RACE cDNA amplification kit (Clontech Laboratories Inc., Mountain View, CA) according to the manufacturer's instructions. Amplification products were analyzed by electrophoresis on 1.5% agarose gels.

Quantitative RT-PCR

Quantitative RT-PCR was performed on a total of 23 cases (Table 1) to assess altered expression of candidate genes close to breakpoints BCL2 associated factor 1 (*BCLAF1* localized to 6q23.3) (in17 cases), utrophin (*UTRN*; 6q24) (in 17 cases), pleiomorphic adenoma gene-like 1 (*PLAGL1*; 6q24) (in 23 cases), collagen type XII α chain 1 (*COL12A1*) (in 19 cases), and GTPase activating Rap/RanGAP domain-like 4 (*GARNL4*; 17p13.3) (in 18 cases). We chose to assess *BCLAF1* and *GARNL4* expression level because of their involvement in the translocation occurring in CMF22. *COL12A1* was chosen for its location in 6q13. *UTRN* and *PLAGL1* were chosen both for their location on 6q24, a region we found recurrently deleted by array CGH, as well as for their possible function as tumor suppressor genes. Quantitative RT-PCR was performed as described previously.[4] For each gene a 3 log dilution curve using cDNA isolated from placenta as a positive control was included to calculate the relative gene expression levels. Relative expression levels were used in the normalization and statistical analysis. Genes for normalization were previously identified.[4,5] Normalization was based on geometric averaging of these normalization genes.[19] We compared the level of expression in the CMF samples to five samples of articular cartilage and seven samples of growth plate cartilage. Due to the limited amount of material, level of expression of each gene was not assessed in all of the samples. GraphPad Prism software package (GraphPad Software, Inc., La Jolla, CA) was used for running *t*-test to assess significant differences ($P < 0.05$ was considered significant) and drawing dot plot graphs. All primers used in the PCR reactions are listed in Table 3 and were designed with

Table 4. Karyotypes from the Studied Cases

Case	Karyotype
CMF21*	46,XY,del(6)(q15),der(6)t(6;6)(q15;q27)inv(6)(p25q13)
CMF22†	46,XX,t(6;17)(q23;p13)
CMF23*	46,XX,del(6)(q2?1q2?3),add(7)(q21)
CMF28†	46,XY,del(6)(q12),der(6)t(6;10)(p25;p11)t(6;11)(q24;p12),der(10)t(6;10)(q12;p11),der(11)t(6;11)(q24;p12)
CMF29†	46,XY,der(6)t(4;6)(q31;q13),der(13)t(1;13)(q21;q21)
CMF30	46,XY,del(6)(q15q23),del(6)(q1?3q2?5),add(11)(q2?5)
CMF31	46,XY,del(6)(q13),der(6)inv(6)(p24q26)ins(6;6)(q13;q25q13), der(22)t(6;22)(q25;p11)
CMF32‡	46,XY,inv(6)(p25q13)/45,idem,−13,+mar
CMF33‡	48,XX,+der(6)del(6)(p11.2)del(6)(q12),+der(?)t(6;?;2;6)(?q25;?;q37q14.3;p12p25)/49,idem,+der(6),del(13)(q21q33)/96,idemx2
CMF38‡	46,XX,t(6;9)(q25;q22),t(7;12)(q32;q13)
CMF39‡	46,XX,del(3)(q23),t(4;6)(q21;q25)
CMF40‡	46,XY,der(6)inv(6)(p25q23)t(6;6)(q23;q13)/46,idem,tas(3;15)(q29;p13),tas(11;15)(p15;p13),tas(15;21)(p13;p13),r(15)
CMF41‡	46,XX,t(1;6)(p35;q25),inv(9)c/46,idem,t(3;4)(p21;p16)
CMF42‡	46,XY,t(6;9)(q25;q22)
CMF43§	46,XY,del(3)(q23q25),t(5;13)(q15;q1?),del(6)(q24q2?)

*Previously reported.[10]
†Karyotype based on G-banding and COBRA-FISH or COBRA-FISH only (case CMF28).
‡Previously reported.[9]
§Karyotype based on G-banding, COBRA-FISH, and metaphase FISH.

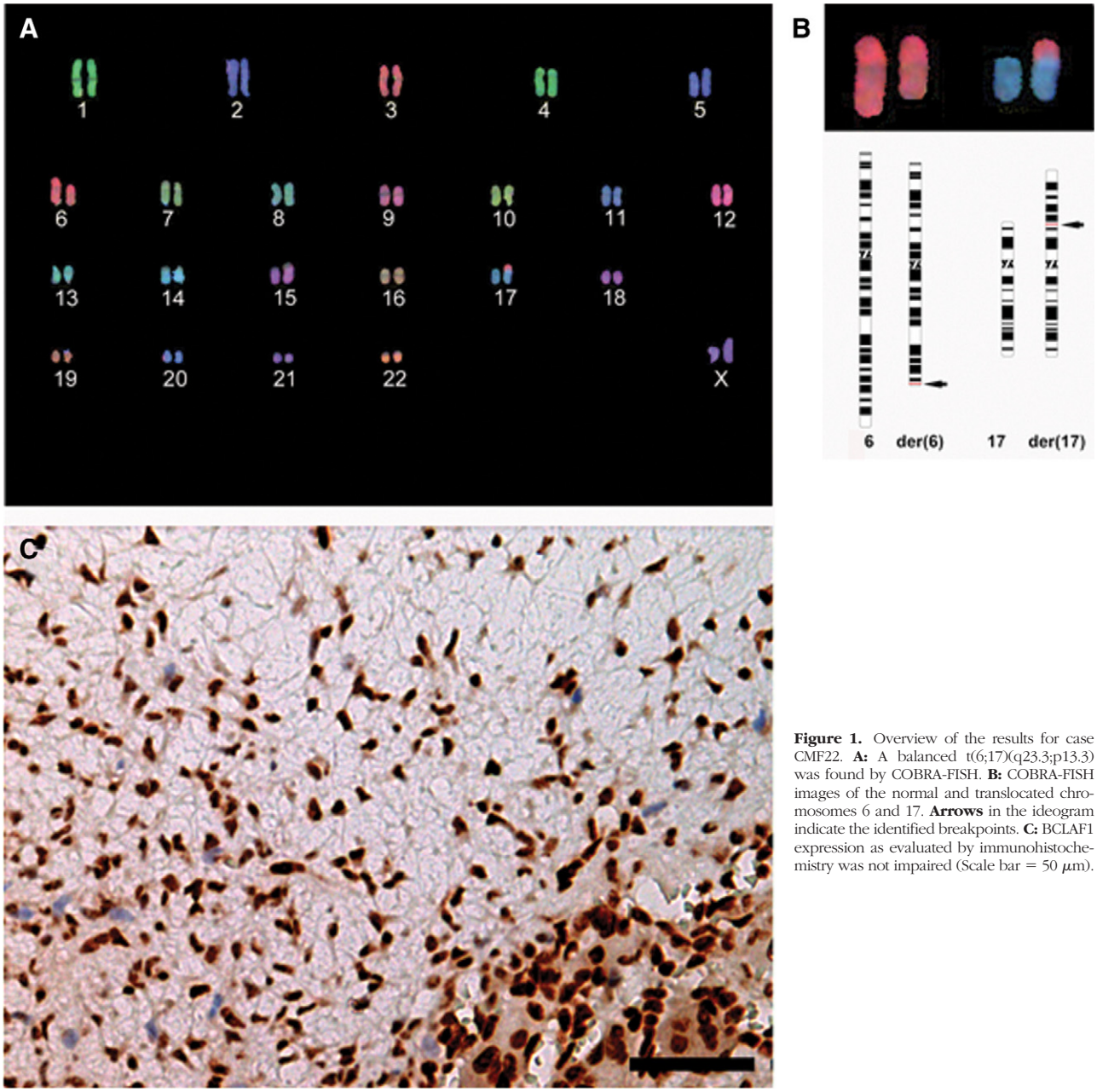

Figure 1. Overview of the results for case CMF22. **A:** A balanced t(6;17)(q23.3;p13.3) was found by COBRA-FISH. **B:** COBRA-FISH images of the normal and translocated chromosomes 6 and 17. **Arrows** in the ideogram indicate the identified breakpoints. **C:** BCLAF1 expression as evaluated by immunohistochemistry was not impaired (Scale bar = 50 μm).

Primer3 (*http://frodo.wi.mit.edu/primer3/input.htm* last accession may 2010).

Immunohistochemistry

To investigate the level and pattern of expression of BCLAF1 and utrophin protein immunohistochemistry was performed on 24 cases (Table 1). Four μm sections of formalin-fixed paraffin-embedded material were used according to standard laboratory procedures.[4] Antigen retrieval was performed by boiling tissue sections in citrate buffer pH 6 in a microwave oven for 10 minutes. Sections from 22 CMFs were then incubated overnight with either anti-BCLAF1 (mouse, monoclonal, clone 5, BD transduction laboratories, Franklin Lakes, NJ, dilution 1:1000) or utrophin (clone 8A4, Novus Biologicals, Littleton, CO, dilution 1:10). Power Vision Plus (Immunological, Duiven, The Netherlands) and 3,3′-diaminobenzidine chromogen (DAB Plus, Dako SA, Glostrup, Denmark) were used for visualization as previously described in detail. The slides were evaluated by two pathologists independently (S.R. and P.C.W.H.) as previously described in detail.[3] The cellular localization (nuclear, cytoplasmic, and membranous) of immunoreactivity was also noted.

Results

Structural Rearrangements of Chromosome 6

Twenty-two cases were cytogenetically analyzed, 15 of which showed abnormal karyotypes. All 15 cases showed

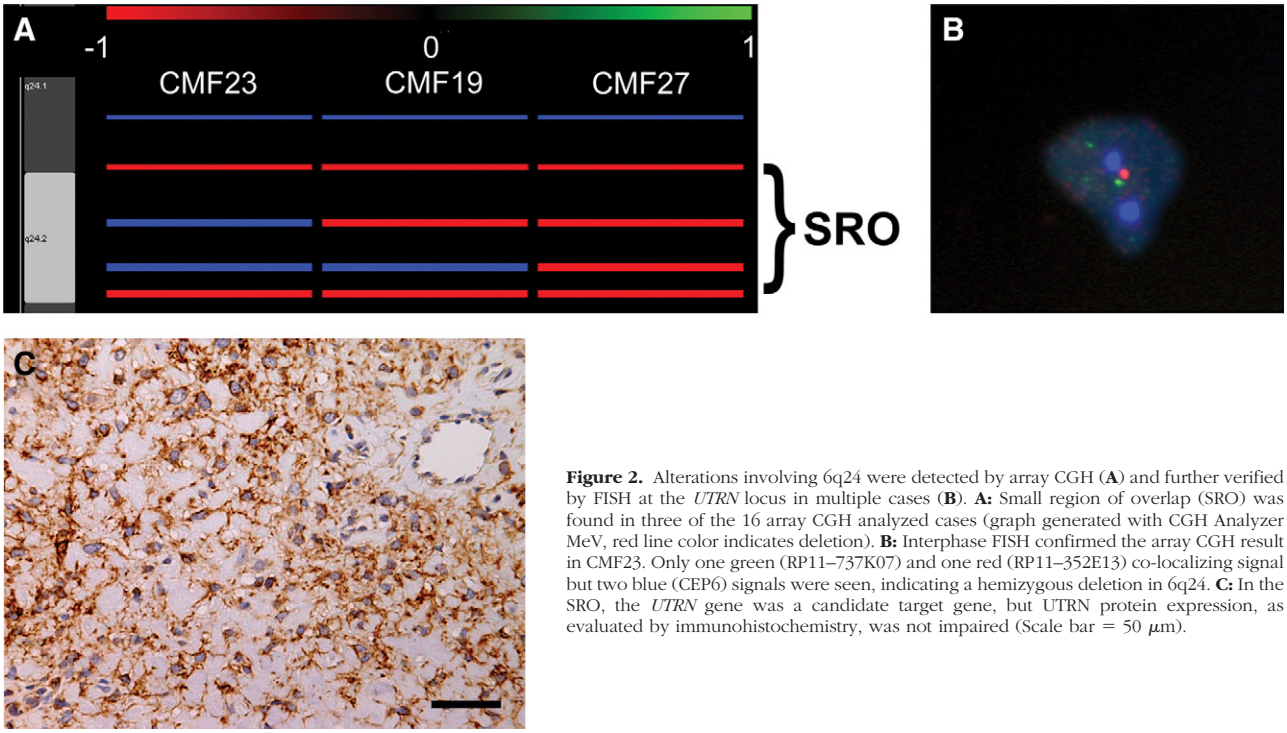

Figure 2. Alterations involving 6q24 were detected by array CGH (**A**) and further verified by FISH at the *UTRN* locus in multiple cases (**B**). **A:** Small region of overlap (SRO) was found in three of the 16 array CGH analyzed cases (graph generated with CGH Analyzer MeV, red line color indicates deletion). **B:** Interphase FISH confirmed the array CGH result in CMF23. Only one green (RP11–737K07) and one red (RP11–352E13) co-localizing signal but two blue (CEP6) signals were seen, indicating a hemizygous deletion in 6q24. **C:** In the SRO, the *UTRN* gene was a candidate target gene, but UTRN protein expression, as evaluated by immunohistochemistry, was not impaired (Scale bar = 50 μm).

aberrations of chromosome 6, with involvement of only the long arm in 10 and both the long and short arms in five (Table 4). Six cases (CMF21, CMF28, CMF30, CMF31, CMF33, and CMF40) showed involvement of both chromosome 6 homologues (Table 4). Six cases (CMF22, CMF32, CMF38, CMF39, CMF41, and CMF42) showed apparently balanced translocations involving one copy of chromosome 6 (Table 4). The remaining cases showed apparently unbalanced rearrangements with involvement of multiple chromosomes and often multiple regions of the long arm of chromosome 6. The results of chromosomal banding analysis were integrated with COBRA-FISH results in five cases (CMF22, CMF28, CMF29, CMF31, and CMF43; Table 4).

Mapping and Cloning of t(6;17)(q23.3;p13.3)

The karyotype of CMF22 was 46,XY,t(6;17)(q23.3;p13.3)-[20]/46,XY[5] (Figure 1, A and B). The breakpoints on chromosomes 6 and 17 were further studied by FISH. The breakpoints were mapped to positions 136.64–136.66 kbp on chromosome 6 and 2.64–2.67 kbp on chromosome 17. Using long-range PCR, a PCR product of approximately 8 kbp was generated, cloned and sequenced. Genomic PCR confirmed the sequence of the translocation and allowed for the amplification of a smaller fragment of 495 bp. The junction on the derivative chromosome 6 occurred at bp positions 136,646,797, within intron 1 of the *BCLAF1* gene, and 2,667,303, within

Table 5. Karyotype after Array CGH According to ISCN 2009

Case	Karyotype
CMF 19	arr cgh 3q13.11 (Rp11-115B22B→RP11-91-B3)X1, 3q13.13(RP11-25F15)X1, 3q13.31 (RP11-572C15→RP11-107J18)X1,3q22.1(RP11-48F15)X1, 3q22.2(RP1122E12)X1,3q25.1q25.2(RP11-145F16→RP11-64O13)X1, 3q25.32q25.33(RP11-53P18→RP11-67-F24)X1, 3q25.1q25.2(RP11-145F16→RP11-64O13)X1, 3q26.1(RP11-198G24)X1,3q26.1q26.2 (RP11-264D7→RP11-141C22B)X1, 3q26.32q27.1(RP11-682A21→RP11-553E4), 3q26.2q26.31(RP11-816J6→RP11-44A1)X1, 3q28(RP11-392H18→RP11-211P13)X1, 6q15(RP1-23D17→RP1-12O8)X1, 6q16.3(RP11-347H8→RP1-244F1)X1, 6q21q22.1(RP1-142L7→RP11-346K2)X1, 6q22.1q22.31(RP1-230I3→RP1-87H18)X1, 6q22.31q22.32(RP1-84N20)X1, 6q24.2(RP11-86O4)X1, 6q24.2 (RP11-386H19)X1
CMF 23	arr cgh 6q22.31q23.2 (RP11-593A16→RP11-295F4)X1, 6q24.1q24.2 (RP11-368P1)X1,6q24.2 (RP11-386H19)X1, 6q25.1q25.2(RP3-443C4→RP1-130E4)X1, 7p13(RP5-1022I14)X1, 7q11.21 (RP5-905H7→RP4-736H5)X1, 7q11.22(RP11-3P22)X1, 7q11.22q11.23(RP11-409J21→RP11-107L23)X1, 7q11.23 (RP467H10)X1, 7q11.23q21.11(RP11-538P15→RP11-343J14)X1,7q21.11(RP11-575G1→RP4-784G16)X1,7q21.11 (RP11-313H6)X1, 7q21.11(RP5-1136A10→RP11-28121B)X1, 7q21.11(RP11-533L22)X1,7q21.2 (RP5-1099C19)X1, 7q21.3 (RP11-95A10→RP5-1145A22)X1,7q22.1(RP4-550A13→RP11-333G13)X1, 7q22.3 (RP11-17I10B→RP11-17I10)X1, 7q31.2(CTB-1013N12→RP11-374M7)X1, 7q31.31(RP11-126C19B→RP11-126C19)X1,7q31.321(RP5-902E20→RP11-264K23)X1, 7q35(RP11-302C22)X1
CMF 27	arr cgh 6q24.1q24.3 (RP11-368P1→RP11-545I5)X1

intron 2 of the *GARNL4* gene, on chromosomes 6 and 17, respectively (GenBank accession number: GQ912699) (according to hg18 at *http://genome.ucsc.edu*, last accessed on December 23, 2009). Despite the intragenic breakpoints no fusion products were generated by RT-PCR using various primer combinations or RACE PCR (data not shown). We were not able to amplify the junction on the derivative chromosome 17, possibly due either to the presence within this region of both short interspersed nuclear element class of repeats as well as long interspersed nuclear element class of repeats, or to the occurrence of more complex genetic events.

Evaluation of Additional Copy Number Changes

Array CGH was performed to identify copy number changes. Copy number loss was found in three of 16 cases: CMF19, CMF23, and CMF27. Complex interstitial deletions were found in two cases, involving chromosomes 3 and 6 (CMF19) and chromosomes 6 and 7 (CMF23), respectively. A deletion was also found in 6q24 in CMF27. Deleted regions ranged in size from 1.6 to 14 Mbp. At chromosome band 6q24 there was a small ~4 Mbp region of overlap, bracketed by BACs RP11-368P1 and RP11-545I5, in three cases (Figure 2, A and B). Four known genes map to this region: *UTRN*, *STX11, EPM2A,* and *PLAGL1*. None of the cases showed homozygous deletion or amplification.

The results of the array CGH analysis complemented and clarified the previous cytogenetic findings (Table 5). For instance, the add(7)(q21) in CMF23 was shown to contain multiple interstitial deletions (Tables 4 and 5). Intriguingly, the complex karyotypic rearrangements in CMF21, CMF28, and CMF31 were not associated with any unbalanced rearrangements at the present resolution of array CGH.

Evaluation of Rearrangements in the Identified Breakpoints (6q13, 6q23.3, 6q24)

By interphase and metaphase FISH the involvement of three recurrent breakpoint regions, 6q13, 6q23.3, and 6q24, was investigated in 29 CMF samples. The selected regions were based on results previously reported by Yasuda et al,[8] the breakpoint identified in CMF22, and the common minimal deleted region found by array CGH, respectively.

Probe sets were generated to detect both copy number alterations and translocations (Table 2). Of the 30 samples, 17 did not show any alterations with the three different probe sets. In the remaining 13 cases four patterns of alteration could be recognized: split signals for one region, hemizygous deletion of one region, hemizygous deletion of all three probe regions (CMF29), and copy number gain in one region (6q23.3 in CMF33; Table 6). Split signals were seen only for the 6q13 and 6q23.3 regions. Translocation breakpoints around the *BCLAF1* locus in the 6q23.3 region, as observed in the index case (CMF22) with a t(6;17), were found in CMF30 and CMF35; in neither of these two cases was chromosome 17 involved. Interstitial hemizygous deletion of one region was seen only for 6q24, in the three cases previously identified by array CGH and in CMF43. A hemizygous deletion of 6q13 was found together with split signals for the 6q23.3 probe set in CMF30.

One case (CMF31) showed complex, biallelic rearrangements of all three investigated regions (Table 6 and Figure 3, A and B). One derivative chromosome 6 was deleted at 6q13. Part (6q25-qter) of the deleted material was translocated to chromosome 22, and part (6q13-q25) of it was inversely inserted into the other der 6 which also had a pericentric inversion with breakpoints in 6p24 and 6q26. The 6q13 break occurred within the set of proximal probes, not including the distal part of RP1–238D15, as it has a significant overlap with the first green probe (Table 2). The FISH revised karyotype of

Table 6. Overview of FISH Analyses for Candidate Breakpoint Regions at Bands 6q13, 6q23.3, and 6q24 Correlated to Karyotype Rearrangements and Array CGH Results

Name	6q13	6q23.3	6q24	Karyotype	Array CGH
CMF2	N	N	N	NP	N
CMF3	N	N	N	NP	N
CMF5	N	N	N	NP	NP
CMF9	NP	N	N	NP	N
CMF11	NP	N	N	NP	N
CMF13	N	N	N	NP	N
CMF19	N	N	HD	NP	DEL
CMF20	N	N	N	NP	N
CMF21	N	N	N	Biallelic, complex, only 6	N
CMF22	NP	SA	N	Monoallelic, balanced	N
CMF23	N	N	HD	HD	DEL
CMF24	NP	N	N	NP	N
CMF25	N	N	N	N	N
CMF26	N	N	N	N	N
CMF27	N	N	HD	N	DEL
CMF28	SA	N	N	Biallelic, complex	N
CMF29	HD	HD	HD	HD	NP
CMF30	HD	SA	N	Biallelic, complex	NP
CMF31	SA/CO*	N*	N*	Biallelic, complex	N
CMF32	SA†	N	N	Monoallelic, complex	NP
CMF33	N†	EG	N	Complex, involving more copies of 6	NP
CMF34	N†	N	N	N	NP
CMF35	N†	SA	N	N	NP
CMF36	N†	N	N	N	NP
CMF37	N†	N	N	N	NP
CMF38	N†	N	N	Monoallelic, balanced	NP
CMF39	N†	NP	NP	Monoallelic, balanced	NP
CMF40	SA†	NP	NP	Biallelic, complex	NP
CMF42	NP	N	N	Monoallelic, balanced	NP
CMF43	N	N	HD	Monoallelic, HD	

*See in Figure 3 one detailed description on metaphase chromosomes.
†Already reported.[9]
N, normal; NP, not performed; SA, split apart; SA/CO, split apart and co-localization; EG, extra green signal without increased centromeric signal (partial trisomy); HD, hemizygous deletion loss of both green and red signal for one allele.

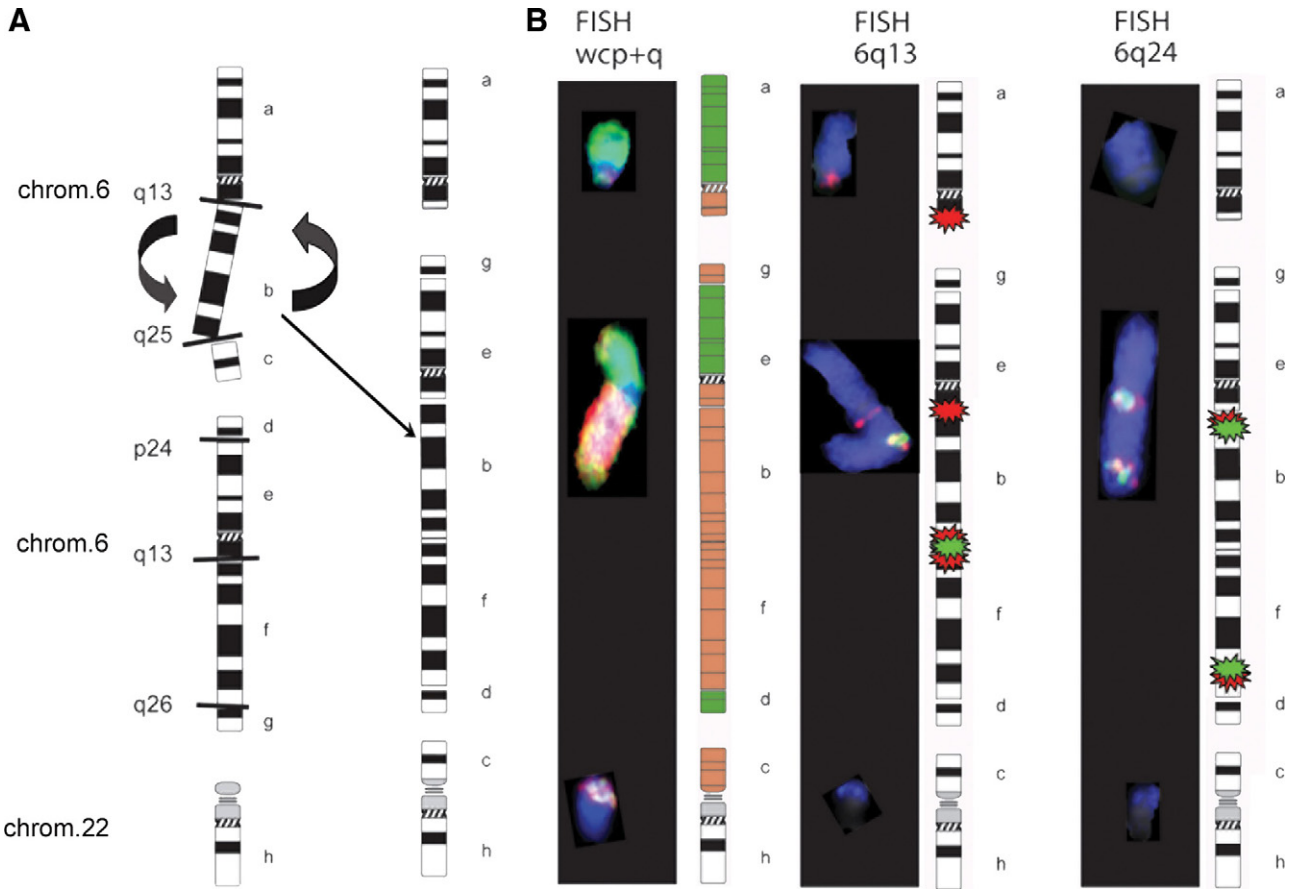

Figure 3. G-banding analysis of CMF31 showed complex rearrangements of both chromosome 6 homologues and one chromosome 22: 46,XY,del(6)(q13), der(6)add(6)(p25)t(6,6)(q2?5;q2?1),add(22)(p11). FISH analysis provided greater detail giving rise to the revised karyotype 46,XY,del(6)(q13),derinv(p24q26)ins(6; 6)(q13;q25q13), der(22)t(6,22)(q25;p11). **A: Left**, ideogram of normal chromosomes 6 and chromosome 22; identified breakpoints are indicated by lines. **Right**, ideograms of the observed rearrangements. Involved chromosome segments are annotated from a to h. **B:** Representative metaphase FISH experiments. **Left**, whole chromosome painting for chromosome 6 (green) in combination with a chromosome arm 6q-specific microdissected library (red) identifies the involved chromosome arms. One derivative chromosome 6 was deleted at 6q13. Part (6q25-qter) of the deleted material was translocated to chromosome 22, and part (6q13–q25) of it was inversely inserted into the other der(6), which also had a pericentric inversion with breakpoints in 6p24 and 6q26. **Middle**, images for 6q13 (proximal region in red and distal region in green, wcp6 in blue) show that the breakpoint between segments a and b occurred within the proximal region covered by the 6q13 probe set. **Right**, the breakpoint between segments b and c was distal to the 6q24 probe set (proximal probe in red, distal probe in green, wcp6 in blue).

CMF31 was 46,XY,del(6)(q13),der(6)inv(6)(p24q26)ins(6; 6)(q13;q25q13), der(22)t(6,22)(q25;p11) (Figure 3).

Evaluation of the Expression of Candidate Genes

No significant changes in expression levels were seen for *BCLAF1*, *GARNL4*, *UTRN, COL12A1,* or *PLAGL1* by qRT-PCR when compared with non-neoplastic cartilage samples from growth plate and articular cartilage (Figure 4). Nor did immunohistochemistry for BCLAF1 and utrophin show any differences between neoplastic and normal cells within the same evaluated sections, or between cases with and without rearrangement of the regions harboring the genes under study (Figures 1C and 2C).

Discussion

We studied 43 CMFs with chromosome banding analysis complemented by multicolor FISH karyotyping, array CGH, breakpoint mapping by FISH with interphase FISH verification, PCR, and immunohistochemistry to identify important underlying genetic mechanisms and examine the expression levels of candidate genes and their proteins.

Karyotypes from 15 cases showed involvement of chromosome 6 with mostly complex rearrangements. One index case harbored a t(6;17)(q23;p13). We performed array CGH to identify non-randomly gained or lost chromosomal regions. Remarkably, most of the CMFs, including those with apparently unbalanced karyotypic changes, did not show any imbalances with array CGH. However, a recurrent deletion in 6q24 was found in three cases. The two candidate target regions identified in our study, namely 6q23.3 and 6q24, as well as the recently implicated region in 6q13,[8] were then selected for further analysis.

Rearrangements of 6q23.3 were detected in five cases: a hemizygous deletion as part of a large deletion in one case (CMF29), a partial gain in one (CMF33), and a translocation in three (CMF22, CMF30,

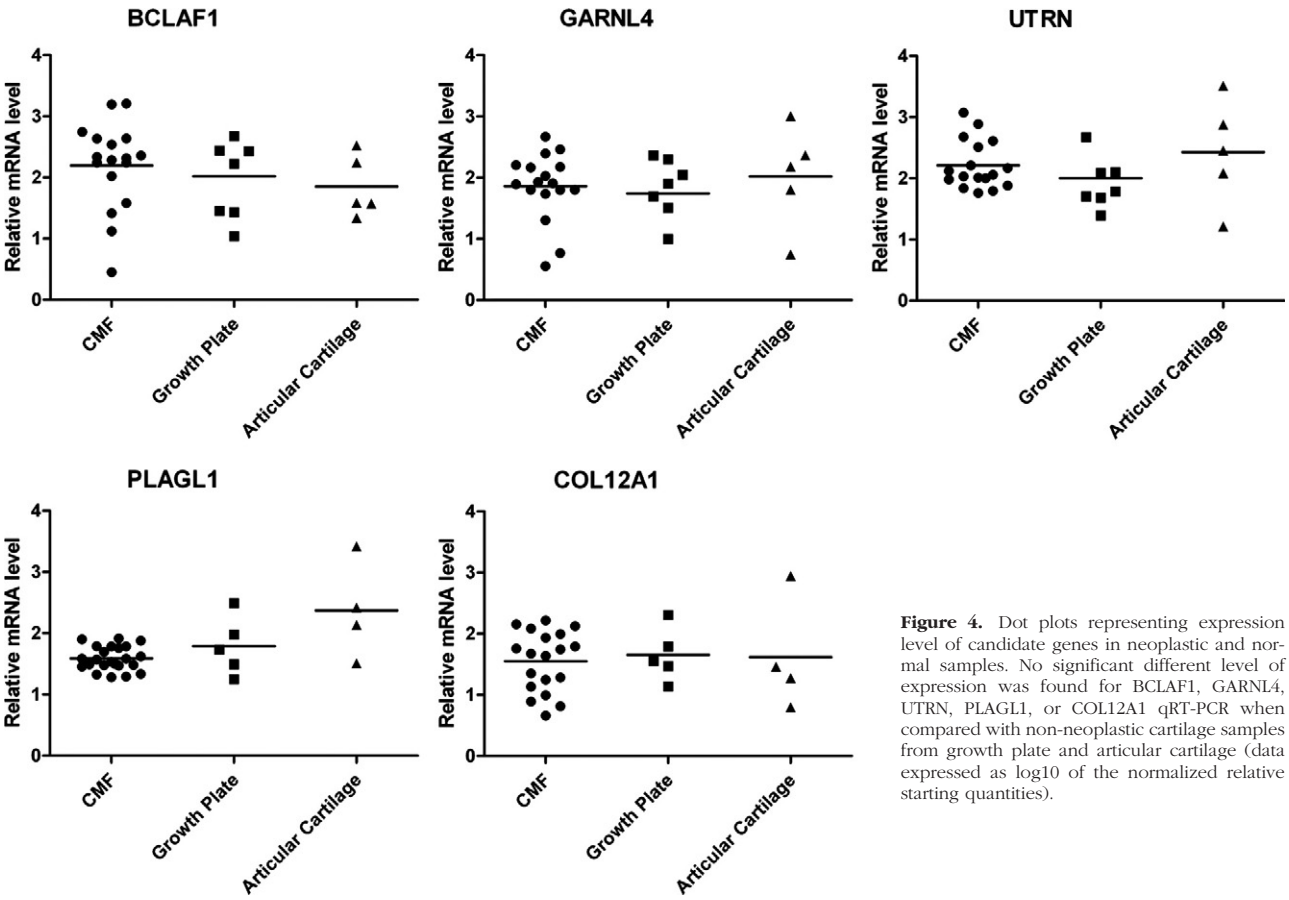

Figure 4. Dot plots representing expression level of candidate genes in neoplastic and normal samples. No significant different level of expression was found for BCLAF1, GARNL4, UTRN, PLAGL1, or COL12A1 qRT-PCR when compared with non-neoplastic cartilage samples from growth plate and articular cartilage (data expressed as log10 of the normalized relative starting quantities).

and CMF35). In agreement with the results of the G-banding, the translocation observed in CMF30 is most likely resulting in translocation to the long arm of chromosome 11. Next, the level of expression of the genes involved in the t(6;17)(q23.3;p13) were assessed. As *BCLAF1* overexpression has been suggested to promote apoptosis,[21] its down-regulation might favor cell growth/survival. However, no significant difference in expression levels was seen for BCLAF1 at the mRNA or protein levels. Lastly, the characterization of the t(6;17)(q23.3;p13) showed that the breakpoints occurred within intron 1 of *BCLAF1* (6q23.3) and intron 2 of *GARNL4* (17p13.3). Although the orientation of these two genes is such that a simple translocation could give rise to a functional fusion transcript, no chimeric mRNA was detected. Thus, either the fusion transcript is promptly degraded or it is not transcribed at all and therefore unlikely to play a role in the pathogenesis of CMF. The latter conclusion is supported by the absence of similar t(6;17) in previously published cases of CMF ((Mitelman Database of Chromosome Aberrations in Cancer (*http://cgap.nci.nih.gov/Chromosomes/* 2009).[6–8]

A hemizygous deletion of 6q24 was found in five cases; in one (CMF29) as part of a larger deletion which also affected the 6q13 and 6q23.3 regions, and as an isolated interstitial deletion in four other cases. Interstitial deletions might have the same functional consequences as a chromosomal translocation. In fact, this can cause the juxtaposition of two genes leading to possible chimera formation or promoter swapping. Deletions may also result in inactivation of genes, and it could be noted that the 6q24 region is reported to be deleted in several other tumors.[18] Two candidate tumor suppressor genes map to 6q24: *UTRN* and *PLAGL1*.[18,21] The level of expression of these two genes was, however, not altered in cases with deletion of this region, suggesting that haploinsufficiency alone of *PLAGL1* or *UTRN* is not of pathogenetic significance in CMF. For case CMF29 it is difficult to speculate on the consequence of a large 6q deletion. However, it should be noted that even germline interstitial deletions in 6q have been reported to occur without apparent phenotypic alterations.[22]

Recently, Yasuda et al[8] mapped a recurrent breakpoint in CMF to 6q13, possibly affecting the collagen type XII α 1*(COL12A1)* locus in three of 14 studied cases. By increasing the study size we found one more case with a translocation, one case with a hemizygous deletion together with a split signal for 6q23.3, one case with hemizygous deletion of all investigated regions, and one case (CMF31) with more complex changes. In the latter case, a breakpoint occurred in the proximal 6q13 region, most likely outside *COL12A1*. By reviewing the given probe map sequence, as reported by Yasuda et al,[9] we discovered discrepancies between the initially reported size and the recently revised size. As the length of BAC RP11-209D8 is not 10,206 bp but 166,681 bp, there is an overlap of 48,892 bp between the distal and proximal

probe. This mismapping might have led to erroneous conclusions on the possible locations of the exonic breakpoints. To clarify whether an involvement of 6q13 region may interfere with *COL12A1* expression , we performed qRT-PCR. *COL12A1* was found to be expressed in CMF, but to a level not significantly different from the one observed in non-neoplastic cartilage form articular surfaces and from growth plate. Rearrangement of one or more of the three breakpoint regions studied here was found in less than 50% of the studied cases. Furthermore, the rearrangements were heterogeneous, and manifested as split signals, lost signals, or even extra signals. Thus, the use of a single probe set as an adjunct diagnostic tool would have a low sensitivity, and the interpretation would be hampered by the heterogeneity of the rearrangements. Finally, the specificity of the use of a single FISH probes set or of a combination of sets should be further evaluated in a large series of cartilaginous tumors. In fact chromosomal arm 6q is often rearranged, especially in chondrosarcomas (Mitelman Database of Chromosome Aberrations in Cancer, *http://cgap.nci.nih.gov/Chromosomes/* 2009).[23–26]

Despite the extensive analyses performed, the mechanisms underlying the genesis of CMF remains elusive. A transcriptomic approach might be helpful, combining wide genome scale expression profiling and microRNA profiling with the observed genetic changes. We have interrogated our gene expression dataset previously generated on CMF[5] to elucidate an altered expression of genes located on chromosome 6. We did not find any significant altered expression (data not shown). However more recent expression profiling platforms might be more sensitive. The genetic changes observed in CMF may be secondary to either a cryptic translocation beyond the detection level of even high resolution multicolor FISH or to a point mutation occurring in a highly vulnerable chromosomal region. Such changes might be identifiable by recently developed technology such as massive sequencing.[27,28]

Acknowledgments

We acknowledge the expert technical work of Jeroen Knijnenburg, Marja van der Burg, and Marije IJszenga (Department of Molecular Cell Biology, Leiden University Medical Center, Leiden, The Netherlands) and Hans J. Baelde and Marcel G.T. Winter (Department of Pathology, Leiden University Medical Center, Leiden, The Netherlands).

References

1. Romeo S, Hogendoorn PCW, Dei Tos AP: Benign cartilaginous tumors of bone: from morphology to somatic and germ-line genetics. Adv Anat Pathol 2009, 16:307–315
2. Ostrowski ML, Spjut HJ, Bridge JA: Chondromyxoid fibroma. World Health Organization Classification of Tumours: Pathology and Genetics of Tumours of Soft Tissue and Bone. Edited by Fletcher CDM, Unni KK, and Mertens F. Lyon, IARC Press, 2002, pp 243–245
3. Romeo S, Bovée JVMG, Grogan S, Taminiau AHM, Eilers PHC, Cleton-Jansen AM, Mainil-Varlet P, Hogendoorn PCW: Chondromyxoid fibroma resembles in vitro chondrogenesis, though differs in expression of signalling molecules. J Pathol 2005, 206:135–142
4. Romeo S, Eyden B, Prins FA, Briaire-de Bruijn IH, Taminiau AHM, Hogendoorn PCW: TGF-beta1 drives partial myofibroblastic differentiation in chondromyxoid fibroma of bone. J Pathol 2006, 208:26–34
5. Romeo S, Oosting J, Rozeman LB, Hameetman L, Taminiau AH, Cleton-Jansen AM, Bovée JVMG, Hogendoorn PCW: The role of noncartilage-specific molecules in differentiation of cartilaginous tumors: lessons from chondroblastoma and chondromyxoid fibroma. Cancer 2007, 110:385–394
6. Armah HB, McGough RL, Goodman MA, Gollin SM, Surti U, Parwani AV, Rao UN: Chondromyxoid fibroma of rib with a novel chromosomal translocation: a report of four additional cases at unusual sites. Diagn Pathol 2007, 2:44
7. Smith CA, Magenis RE, Himoe E, Smith C, Mansoor A: Chondromyxoid fibroma of the nasal cavity with an interstitial insertion between chromosomes 6 and 19. Cancer Genet Cytogenet 2006, 171:97–100
8. Yasuda T, Nishio J, Sumegi J, Kapels KM, Althof PA, Sawyer JR, Reith JD, Bridge JA: Aberrations of 6q13 mapped to the COL12A1 locus in chondromyxoid fibroma. Mod Pathol 2009, 22:1499–1506
9. Tallini G, Dorfman H, Brys P, Dal Cin P, De Wever I, Fletcher CD, Jonson K, Mandahl N, Mertens F, Mitelman F, Rosai J, Rydholm A, Samson I, Sciot R, Van den Berghe H, Vanni R, Willen H: Correlation between clinicopathological features and karyotype in 100 cartilaginous and chordoid tumours: a report from the Chromosomes and Morphology (CHAMP) Collaborative Study Group. J Pathol 2002, 196:194–203
10. Granter SR, Renshaw AA, Kozakewich HP, Fletcher JA: The pericentromeric inversion, inv (6)(p25q13), is a novel diagnostic marker in chondromyxoid fibroma. Mod Pathol 1998, 11:1071–1074
11. Sjogren H, Orndal C, Tingby O, Meis-Kindblom JM, Kindblom LG, Stenman G: Cytogenetic and spectral karyotype analyses of benign and malignant cartilage tumours. Int J Oncol 2004, 24:1385–1391
12. Safar A, Nelson M, Neff JR, Maale GE, Bayani J, Squire J, Bridge JA: Recurrent anomalies of 6q25 in chondromyxoid fibroma. Hum Pathol 2000, 31:306–311
13. Polito P, Dal Cin P, Debiec-Rychter M, Hagemeijer A: Human solid tumors: cytogenetics techniques. Methods in Molecular Biology. Cytogenetics: Methods and Protocols. Edited by GJ Swansbury. Totowa, NJ, Humana Press, 2003, 220:135–150
14. Szuhai K, Tanke HJ: COBRA: combined binary ratio labeling of nucleic-acid probes for multi-color fluorescence in situ hybridization karyotyping. Nature Protocols 2006, 1:264–275
15. Knijnenburg J, van der Burg M, Nilsson P, Ploos van Amstel HK, Tanke HJ, Szuhai K: Rapid detection of genomic imbalances using micro-arrays consisting of pooled BACs covering all human chromosome arms. Nucleic Acids Res 2005, 33:e159
16. Romeo S, Szuhai K, Nishimori I, Ijszenga M, Wijers-Koster P, Taminiau AHM, Hogendoorn PCW: A balanced t(5;17) (p15;q22–23) in chondroblastoma: frequency of the re-arrangement and analysis of the candidate genes. BMC Cancer 2009, 9:393
17. Greshock J, Naylor TL, Margolin A, Diskin S, Cleaver SH, Futreal PA, deJong PJ, Zhao S, Liebman M, Weber BL: 1-Mb resolution array-based comparative genomic hybridization using a BAC clone set optimized for cancer gene analysis. Genome Res 2004, 14:179–187
18. Li Y, Huang J, Zhao YL, He J, Wang W, Davies KE, Nose V, Xiao S: UTRN on chromosome 6q24 is mutated in multiple tumors. Oncogene 2007, 26:6220–6228
19. Vandesompele J, De Preter K, Pattyn F, Poppe B, Van Roy N, De Paepe A, Speleman F: Accurate normalization of real-time quantitative RT-PCR data by geometric averaging of multiple internal control genes. Genome Biol 2002, 3: research0034.1–0034.11
20. Haraguchi T, Holaska JM, Yamane M, Koujin T, Hashiguchi N, Mori C, Wilson KL, Hiraoka Y: Emerin binding to Btf, a death-promoting transcriptional repressor, is disrupted by a missense mutation that causes Emery-Dreifuss muscular dystrophy. Eur J Biochem 2004, 271:1035–1045
21. Poulin H, Labelle Y: The PLAGL1 gene is down-regulated in human extraskeletal myxoid chondrosarcoma tumors. Cancer Lett 2005, 227:185–191
22. Hansson K, Szuhai K, Knijnenburg J, van Haeringen A, de Pater J:

Interstitial deletion of 6q without phenotypic effect. Am J Med Genet A 143:2007, 1354–1357
23. Rozeman LB, Szuhai K, Schrage YM, Rosenberg C, Tanke HJ, Taminiau AHM, Cleton-Jansen AM, Bovee JVMG, Hogendoorn PCW: Array-comparative genomic hybridization of central chondrosarcoma: identification of ribosomal protein S6 and cyclin-dependent kinase 4 as candidate target genes for genomic aberrations. Cancer 2006, 107: 380–388
24. Bovée JVMG, Royen Mv, Bardoel AFJ, Rosenberg C, Cornelisse CJ, Cleton-Jansen AM, Hogendoorn PCW: Near-haploidy and subsequent polyploidization characterize the progression of peripheral chondrosarcoma. Am J Pathol 2000, 157:1587–1595
25. Bovée JVMG, Sciot R, Dal Cin P, Debiec-Rychter M, Van Zelderen-Bhola SL, Cornelisse CJ, Hogendoorn PCW: Chromosome 9 alterations and trisomy 22 in central chondrosarcoma: a cytogenetic and DNA flow cytometric analysis of chondrosarcoma subtypes. Diagn Mol Pathol 2001, 10:228–236
26. Buddingh EP, Naumann S, Nelson M, Neffa JR, Birch N, Bridge JA: Cytogenetic findings in benign cartilaginous neoplasms. Cancer Genet Cytogenet 2003, 141:164–168
27. Stephens PJ, McBride DJ, Lin ML, Varela I, Pleasance ED, Simpson JT, Stebbings LA, Leroy C, Edkins S, Mudie LJ, Greenman CD, Jia M, Latimer C, Teague JW, Lau KW, Burton J, Quail MA, Swerdlow H, Churcher C, Natrajan R, Sieuwerts AM, Martens JW, Silver DP, Langerod A, Russnes HE, Foekens JA, Reis-Filho JS, van 't Veer L, Richardson AL, Borresen-Dale AL, Campbell PJ, Futreal PA, Stratton MR: Complex landscapes of somatic rearrangement in human breast cancer genomes. Nature 2009, 462:1005–1010
28. Stratton MR, Campbell PJ, Futreal PA: The cancer genome. Nature 2009, 458:719–724